ARTICLES

Exciton Annihilation in J-Aggregates Probed by Femtosecond Fluorescence Upconversion

Johannes Moll,[†,‡] William J. Harrison,[§] Donald V. Brumbaugh,[†,§] and Annabel A. Muenter*[,†,§]

Center for Photoinduced Charge Transfer, Department of Chemistry, University of Rochester, Rochester, New York 14627, and Imaging Research and Advanced Development Laboratories, Eastman Kodak Company, Rochester, New York 14652-4708

Received: September 7, 1999; In Final Form: July 24, 2000

Femtosecond fluorescence upconversion was used to study the excited-state dynamics of two-dimensional J-aggregates of a thiacyanine dye. At high intensities the excited-state population decay is faster than exponential and the decay is intensity dependent. A singlet−singlet exciton annihilation decay mechanism is consistent with the observed behavior. A value of 4×10^{12} molecule s^{-1} is calculated for the exciton annihilation constant γ. Exciton annihilation measurements reported in the literature for J-aggregates of several cyanine dyes are recast into the same units for comparison. The physical state of these J-aggregates is elucidated to explore the relationship between the magnitude of the exciton annihilation constants and the liquid-crystalline nature of these aqueous colloidal systems. Attempts to time-resolve spectral features related to intraband relaxation in the excited excitonic states of the thiacyanine J-aggregate prior to annihilation indicate that these relaxation processes are faster than 100 fs at room temperature.

Introduction

Molecular aggregates, like many other mesoscopic systems, have attracted considerable attention in recent years.[1,2] Aqueous ionic dye systems exhibit a marked tendency for molecular self-association as a result of the strong intermolecular van der Waals attractive forces operating between these usually planar, polycyclic molecules. This association is accompanied by alterations in the optical absorption spectra of the solutions, consisting of large spectral shifts and distinct changes in band shape. Species with bands shifted to the blue relative to the monomer absorption are termed H-aggregates while species with red-shifted, narrowed bands are termed J-aggregates.[3] Excitation in the J-aggregate band produces a collective excited state (exciton[4]). The modification and size enhancement of certain optical properties due to the formation of excitons is of particular interest for future nonlinear optical applications. Today, J-aggregates of cyanine dyes are widely used for the spectral sensitization of photographic materials[5] in preference to the nonaggregated monomeric state because they provide both maximum light absorption per silver halide crystal and a narrow selective spectral absorption envelope.

Recent phase behavior studies of representative aqueous ionic dye systems have established that lyotropic liquid crystal ("mesophase") formation occurs at unusually low dye concentrations.[6−9] Both layer (lamellar/smectic) mesophases and columnar (nematic and hexagonal) mesophases have been observed, depending on the structure of the dye. For a number of aqueous cyanine dyes, the concentration onset of these anisotropic supramolecular mesophases has been shown to coincide with the appearance of the characteristic excitonic J-band.[7,10]

Many aspects of the formation, evolution, and decay of excitons in molecular aggregates are still not completely understood. It is known that before the exciton decays by emission of a photon or by nonradiative processes, both coherent and incoherent energy transfer, as well as relaxation within the exciton band occur on a femtosecond time scale. Additionally, when the exciton density is sufficiently high, interactions between excitons, in particular exciton−exciton annihilation, can no longer be neglected and lead to dramatic changes in the optical response from the aggregates. Exciton−exciton annihilation is the nonradiative interaction of two excitations in which one or both of the excitations vanish, thus leading to an additional nonradiative depopulation of the excited state and a dramatic change in the fluorescence lifetime and quantum yield. For several years, this effect caused large discrepancies in the reported aggregate lifetimes before picosecond intensity-dependent measurements revealed the origin of these differences.[11−13]

In this paper, we present new data on J-aggregate exciton annihilation in a thiacyanine dye as obtained from femtosecond fluorescence upconversion experiments and compare our results to previous measurements of exciton annihilation in other J-aggregated cyanine dyes. In addition, we examine whether the ∼100 fs time scale of our experiments is sufficient to resolve the intraband exciton relaxation occurring prior to exciton annihilation. To assess the influence of dye liquid crystal formation on exciton dynamics, we have also investigated the solution phase behavior of the comparative J-aggregated dye systems.

[†] Center for Photoinduced Charge Transfer.
[‡] Present address: Corning Incorporated, Sullivan Park, SP-DV-02, Corning, NY 14831.
[§] Imaging Research and Advanced Development Laboratories.

10.1021/jp993154d CCC: $19.00
Published on Web 09/07/2000

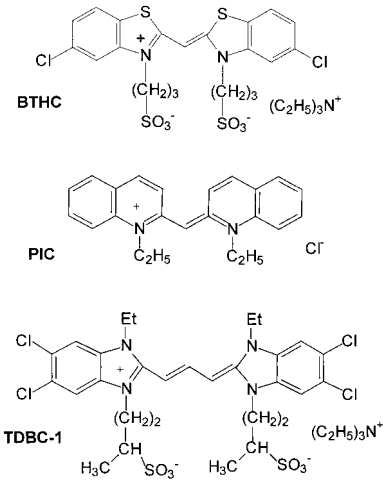

Figure 1. Chemical structures of BTHC, PIC, and TDBC-1.

Experimental Section

The dyes BTHC, PIC, and TDBC-1 (Figure 1) were synthesized at the Research Laboratories of Eastman Kodak Company. For BTHC, the sample used for spectroscopic studies was prepared by dissolving the dye in distilled water and adding an aqueous solution of NaCl, resulting in a solution with a dye concentration of 6.5×10^{-5} M and a salt concentration of 0.15 M. For PIC, NaCl to a concentration of 0.2 M was added to a 3×10^{-4} M aqueous solution of the dye, to reproduce the conditions described by Sundström et al.[13] For TDBC-1, a 5×10^{-5} M aqueous dye solution containing 1×10^{-3} M NaOH (to adjust pH to 11.0) was used to replicate the TDBC dye system studied by van Burgel et al.[14] (Note that our triethylammonium TDBC-1 dye salt has the same chromophore as the van Burgel sodium TDBC dye but is not structurally identical, as TDBC bears n-sulfopropyl, rather than 4-sulfobutyl, substituents on the heterocyclic nitrogens.) More concentrated aqueous solutions of all three dyes, both with and without added salt, were also prepared to examine and compare the phase behavior and mesophase properties of each dye.

Polarized-light optical microscopy observations of aqueous dye films were performed with a Vickers M41 Photoplan polarizing microscope at a magnification of 16X objective. Concentrated dye samples were contained between standard glass microscope slides and coverslips while dilute solutions were sealed in quartz spectrophotometer cells (1 mm path length). Liquid crystal formation was surveyed initially for each dye using the so-called "solvent penetration technique". Here, water (or aqueous salt solution) was allowed to diffuse into the solid dye, confined between a slide and coverslip, to establish a concentration gradient across the sample. Characteristic mesophase textures may then be identified as separate flowing birefringent bands around the solid dye.[6] To supplement the microscopic observations, macroscopic visual observations in polarized light were performed on dye solutions of known composition sealed in 1 mm quartz cells or glass vials.

The femtosecond fluorescence upconversion experiments (Figure 2) were performed using a mode-locked titanium−sapphire-laser (Ti:Sa-Laser) pumped by an argon-ion-laser (Ar^+−Laser). The Ti:Sa produced pulses at 82 MHz, 850 mW (10 nJ/pulse), and 850 nm (spectral width ca. 15 nm). The light from the laser was frequency-doubled using a 0.25 mm BBO crystal, yielding about 60 mW (0.75 nJ/pulse) of 425 nm blue light. The blue light was separated from the remaining fundamental (gate) with a harmonic beam splitter, directed over a computer-controlled delay line, and focused onto the sample.

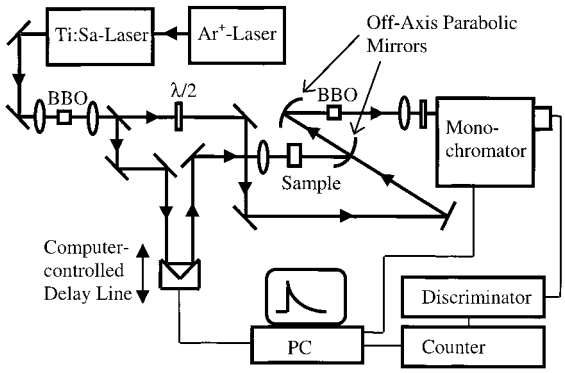

Figure 2. Fluorescence upconversion apparatus (see text for details).

The sample consisted of dye solution flowing through a 100 μm quartz flow cell at 125 mL/min. The average diameter of the laser beam in the sample was estimated to be 10 μm. Polarization of the laser beam was aligned parallel to the flow direction. Note, however, that measurement of the dye absorption spectrum under identical flow conditions indicated no difference in absorption for light polarized parallel or antiparallel to the flow direction. The sample fluorescence was collected and focused on a 0.25 mm BBO-crystal using two off-axis parabolic mirrors. The gate beam was directed through a hole in the first parabolic mirror and also focused on the BBO crystal by the second parabolic mirror. The BBO-crystal was angle-tuned for mixing the gate beam with the sample fluorescence. The resulting UV light was isolated using filters and a monochromator and detected with a photomultiplier tube. The signal pulses were counted using a discriminator and a counter and timer. The cross-correlation of the exciting blue beam and the gate beam in our setup is approximately Gaussian-shaped and has a full width at half-maximum (fwhm) of 220 fs. The incident excitation intensity was varied between 3×10^{13} and 2.15×10^{15} photons pulse^{-1} cm^{-2} by moving the first crystal (where the infrared beam from the Ti:Sa is frequency-doubled) in and out of focus, changing the efficiency of the second harmonic generation and thus the intensity of the blue light used for exciting the sample fluorescence. The time-evolution of the fluorescence at 470 nm, the J-band peak, was measured by scanning the delay line over a distance that corresponds to a time-window of 100 ps in steps of 500 fs; the signal was accumulated for 10 to 30 s at each point. For these data, the measured decay was not deconvoluted but fitted directly because the system cross-correlation time is shorter than a single step in the scan. For studies of the time evolution of the fluorescence at very short times, the time evolution of the fluorescence and the cross-correlation were measured as described above, but with a step size of 100 fs. In this case, the experimental data were then fitted by numerically convoluting the theoretical decay (eq 1, see below) with the experimentally determined cross-correlation function.

For the time-correlated single photon counting (TCSPC) experiments the laser system consisted of a cavity-dumped dye laser synchronously pumped by the second harmonic of a cw mode-locked Nd:YLF laser. The output of the dye laser was mixed with the fundamental of the Nd:YLF laser to obtain laser pulses at 427 nm, which were used for excitation of the fluorescence. The fluorescence from the samples was detected behind a 0.25 m monochromator using a Hamamatsu R3809U-01 microchannel plate. The signal was then amplified and routed through a constant fraction discriminator and time-to-amplitude converter (TAC) as a start-pulse (the stop pulse was triggered by the subsequent laser pulse). The TAC output was analyzed

by a multichannel pulse height analyzer and then saved on a desktop computer. The decay curves were then deconvoluted using a program from Edinburgh Instruments, which is based on the Levenberg−Marquardt algorithm.

Results and Discussion

Phase Behavior of J-Aggregated Dyes. In water, the anionic cyanine dye BTHC forms a J-aggregated smectic mesophase over a finite range of concentration and temperature.[6,7] Here, the individual mesogenic J-aggregates are "infinitely extending" two-dimensional (2D) dye monolayer sheets. An illustration of the spectral changes accompanying the formation of these J-aggregates can be found in ref 6. At very low concentrations ($\leq 1 \times 10^{-6}$ M), the dye is present in solution mainly as the monomer, absorbing at 428 nm. As the concentration is increased, the blue-shifted H-aggregate band (probably a dimeric species) forms at 406 nm in equilibrium with the monomer but the solution remains isotropic. With further increases in dye concentration, the first-order transition from the homogeneous isotropic solution phase to the homogeneous J-aggregate smectic phase proceeds via an intervening heterogeneous two-phase regime (composed of coexisting dye solution and dye liquid crystal), extending from approximately 0.01 to 2.0 wt % dye (% w/w dye, equivalent to 1.4×10^{-4} to 2.9×10^{-2} M dye) at ~25 °C. For BTHC, and other ionic dyes,[15] the addition of monovalent electrolytes may stabilize the mesophase with respect to both concentration and temperature, by reducing short-range electrostatic repulsions between neighboring, close-packed dye molecules within the mesogenic J-aggregates.

In the present study, the addition of 0.15 M NaCl was found to effectively stabilize smectic mesophase (J-aggregate) formation and reduce its concentration onset. For the specific ternary composition reported here (containing 6.5×10^{-5} M, approximately 0.005% w/w BTHC) the heterogeneous 2-phase sample was composed of a dilute swollen smectic mesophase dispersed in almost pure water. Indeed, undisturbed bulk samples were observed to slowly phase separate, yielding a fine, redispersible dye "flocculate" at the bottom of the container. This liquid-crystalline flocculate exhibited a birefringent texture, morphology, and J-band spectral absorption similar to such properties of the salt-free BTHC smectic mesophase formed at correspondingly higher dye concentration. In the absence of NaCl, BTHC dye formed a homogeneous isotropic solution (monomer and H-aggregate equilibrium) at a concentration of 6.5×10^{-5} M in water.

Exciton annihilation in the J-aggregate of the anionic benzimidazole carbocyanine TDBC has been previously measured by van Burgel, Wiersma, and Duppen using a time-resolved grating scattering technique.[14] For the closely related aqueous TDBC-1 system, our polarized-light microscopic and macroscopic observations have revealed an evolutionary phase behavior qualitatively similar to BTHC, and confirmed the smectic liquid-crystalline nature of the J-aggregated state. For TDBC-1, addition of as little as 1.0×10^{-3} M NaOH to a 5×10^{-5} M aqueous dye solution (corresponding to the van Burgel et al. pH 11.0-adjusted TDBC system) apparently stabilized the smectic mesophase at the expense of the coexisting isotropic dye solution of monomers and H-aggregates. In this case, the mesophase (J-aggregate) stability enhancement resulting from such low Na^+ levels may be related more to specific counterion effects (tetraethylammonium cation versus Na^+) rather than a true salt-stabilization effect (indeed similar results were also obtained with 1.0×10^{-3} M additions of both NaSCN and NaCl). In comparison to BTHC, the solution stability of the TDBC-1 smectic mesophase was considerably more sensitive to ionic strength. Addition of 0.15 M NaCl to a 5×10^{-5} M aqueous TDBC-1 solution was found to precipitate the smectic dye mesophase from solution as a solid microcrystalline phase (clearly distinguishable by optical microscopy). Interestingly, the salted-out TDBC-1 solid phase (redispersed by vigorous agitation) was found to exhibit a J-band absorption similar to the aqueous smectic mesophase, although slightly broader and lower in intensity. Similar salting-out effects have been reported for aqueous azo dye mesophases with NaCl.[9]

Exciton annihilation in J-aggregates was first observed in the aggregate of the cationic dye PIC and the dynamics of the process have been measured by several different groups, both in aqueous solution[11−13] and in the presence of poly(vinyl sulfate) polymer.[16] In marked contrast to both BTHC and TDBC-1, PIC (as the chloride salt) forms a thermodynamically stable J-aggregated nematic, rather than smectic, mesophase in aqueous solution,[10] with a concentration onset of approximately 0.18% w/w dye (5.0×10^{-3} M) at ~21 °C. Here the mesogenic J-aggregates are, by inference, long dye columns or stacks rather than "infinite" 2D smectic sheets.[7] Addition of 0.2 M NaCl to an aqueous 3.0×10^{-4} M (0.01% w/w) PIC fluid isotropic solution (to replicate the conditions used by Sundström et al.[13]) was sufficient to promote significant salt-induced columnar aggregate growth as evidenced by the appearance of marked viscoelastic and shear-thinning flow properties. Vigorous agitation of this sample was sufficient to reduce the bulk viscosity to a water-like consistency, consistent with a highly shear-dependent J-aggregate size. The observation of accompanying strong static (nonflowing) fluorescence and birefringence (Schlieren texture) for the undisturbed sample was more consistent with the salt-induced stabilization of a dilute nematic mesophase dispersion, rather than simple columnar aggregate growth in an inherently isotropic solution. (For nematic mesophase-forming dyes such as PIC, it is conceivable that J-aggregate spectral features may be observed for the columnar aggregates in the isotropic solution phase as the mesophase boundary is approached, if aggregate size is a strong function of temperature and concentration. Stegemeyer[10] has reported such a phenomenon for PIC aqueous isotropic solutions some degrees beyond the nematic mesophase melt.) Characteristically, the stability of the PIC nematic liquid crystal compositions studied here (and hence the J-aggregate physical size) were strongly temperature dependent, both with and without salt. For example, our 3.0×10^{-4} M PIC solution with 0.2 M NaCl was found to exhibit a reversible 6-fold increase in J-band intensity at the expense of the coexisting monomer band on decreasing the temperature from ~25 to ~3 °C. This was consistent with an increase in nematic mesophase volume fraction and a concomitant decrease in coexisting isotropic solution with decreasing temperature in this two-phase sample. This is in marked contrast to the aqueous smectic mesophases of BTHC, TDBC-1, and many other smectic-mesophase-forming anionic cyanine dyes,[17] where the phase boundaries delineating the region of mesophase stability are practically vertical with respect to temperature and dye concentration. Here, the first-order phase transition from the isotropic solution phase to the liquid crystal phase may be accompanied by an explosive growth in aggregate size from small H-aggregates directly to supramolecular, infinitely extending, 2D smectic sheets (J-aggregates).

Because of the highly anisotropic nature of the liquid-crystalline J-aggregates compared here, measurements of their physical properties, using for example absorption and fluorescence-based techniques, will be strongly dependent upon

mesophase- (and hence molecular and transition dipole-) orientation effects. Lyotropic liquid-crystalline dye phases exhibit a marked tendency to be aligned by shear flow,[18] in quite different ways depending upon their structural elements, and by surface forces (particularly nematic mesophase-forming dyes such as PIC under short-path-length conditions). Hence, to make valid data comparisons, knowledge of the J-aggregate structure, mesophase-director alignment under the prevailing experimental conditions (e.g., static, dynamic) and mesophase stability (with respect to both dye concentration and temperature) becomes paramount. Additional experimental complications may result from the heterogeneity of these dilute biphasic dye systems and from dye adsorption and J-aggregation on the interior walls of spectrophotometer cells, particularly for dilute, low-volume samples. Furthermore, the observation of J-band spectral features for dyes dispersed in aqueous media (particularly salt-induced J-aggregates) is, in itself, not unequivocal evidence for liquid crystal formation. For example, salt-stabilized mesogenic (liquid-crystalline) J-aggregates are likely to exhibit significantly different physical properties from salt-precipitated microcrystalline (solid) J-aggregated species.

Exciton Annihilation Fundamentals. There are several known models for the effect of exciton annihilation on the fluorescence decay and quantum yield. One model by Paillotin et al.[19] uses a Pauli master equation approach and is based on the assumption that exciton migration is restricted to domains of finite size, but undetermined dimension. It is important to note that the domain size in this model is a physical size confining the exciton within the domain boundaries. This size is not the same as the average number of molecules visited by the exciton in its lifetime (the exciton range), which may be a number considerably smaller than the physical domain size. In the Paillotin model, it is also assumed that the number of molecules over which the exciton is coherently delocalized is small compared to the exciton range, so that the motion of the excitons can be treated as a random hopping process. The parameters of the model are K, the unimolecular fluorescence decay rate in the absence of exciton annihilation; γ, the spatially averaged bimolecular exciton annihilation constant corresponding to disappearance of one exciton per annihilation event; and $n(0)$, the mean number of excitons created per domain at $t = 0$ for a given set of excitation conditions. In formulating their model, Paillotin et al. also introduced the dimensionless parameter $r = 2K/\gamma$, which, for a given pair of excitons, is the ratio of their decay by monoexcitonic processes to their decay by annihilation. As these authors point out, a comparison of experimental data with the general theoretical expression is difficult and fits are usually only feasible in limiting cases: (a) $\gamma \gg 2K(r \rightarrow 0)$: this leads to a very rapid drop in the fluorescence intensity I just after excitation and then an exponential decay with rate K; (b) $\gamma \ll 2K$: this leads to nonexponential decay with

$$I(n(0),t) = \frac{I(n(0),0)}{e^{Kt}(1 + n(0)/r) - n(0)/r} \tag{1}$$

which in the limit of $r \rightarrow \infty$ (no annihilation), as required, approaches an exponential decay with the decay rate K. This equation assumes that processes in which both excitons are annihilated can be neglected, i.e., only $S_1 + S_1 \rightarrow S_1 + S_0$ is considered. Equation 1 is also the solution found for the differential equation used in the binary collision theory:[20]

$$\frac{\partial n(t)}{\partial t} = -Kn(t) - \frac{\gamma}{2} n(t)^2 \tag{2}$$

where the factor of $^1/_2$ results from the assumption that only one of the two participating excitons is annihilated. For the case where r is large, eq 1 can be integrated to give a value for the dependence of the fluorescence quantum yield on excitation density:

$$\Phi(n(0)) = \Phi_0 \frac{r}{n(0)} \ln\left(1 + \frac{n(0)}{r}\right) \tag{3}$$

where Φ_0 is the fluorescence quantum yield in the absence of annihilation. Regardless of the value of r the fluorescence quantum yield in the Paillotin model of restricted domains is given by[19]

$$\Phi(n(0)) = \Phi_0 \sum_{j=0}^{\infty} \frac{(-n(0))^j \Gamma(r+1)}{(j+1)\Gamma(j+r+1)} \tag{4}$$

where Γ is the gamma function.

In these equations, it is assumed that the excitations redistribute sufficiently rapidly that the slope of the fluorescence decay at a time t only depends on $n(t)$ and not on previous events. This assumption may not hold in cases where the dimensionality of the system is reduced or where the excitations are spatially fixed (immobile). In these cases the exciton annihilation rate γ is time dependent $\gamma = \gamma_0 t^{-h}$ with $h = ^1/_2$ for fixed excitations[21] and $h = 1 - d_s/2$ in the case of reduced dimensionality ($d_s \leq 2$).[22] The time dependence disappears for $d_s \geq 2$. d_s is usually referred to as the spectral dimension of a system. In molecular systems it can be used to describe (off-diagonal) disorder. Its values are limited to a range between the system's topological dimension (integer) and the dimension of the embedding Euclidean space,[23] which is 3.

Because BTHC smectic J-aggregates are essentially two-dimensional,[6] i.e., $d_s = 2$, we used the Paillotin model to fit our data. The linear decay rate K was determined in a picosecond time-correlated single-photon-counting (TCSPC) experiment, since the signal amplitude from the upconversion experiment was too low to complete experiments in a reasonable amount of time for the intensity regime where no annihilation occurred. The fluorescence upconversion decays were then fit to eq 1 using the TCSPC determined value of K, yielding values for $n(0)/r$ at different excitation intensities. The resulting good quality of the fits confirmed that, in this case, it is not necessary to consider the effect of restricted dimensionalities.

In principle, the parameter r can be independently determined by fitting the intensity dependence of the experimental fluorescence quantum yield Φ_{exp} using eq 4. Once r is known, the exciton annihilation rate follows from $r = 2K/\gamma$ and a value for $n(0)$ (at a given intensity) follows from the $n(0)/r$ ratios obtained from the fluorescence decay fits. The average domain size D is then the ratio of $n(0)$, the number of excitations per domain, to the fraction of molecules excited:

$$D = \frac{cN_A V}{PA} n(0) \tag{5}$$

(N_A = Avogadro-constant, A = absorption coefficient at the excitation wavelength, c = dye concentration, V = volume of excited sample, P = no. of photons/pulse).

In practice, as will be discussed below, when the domain size is very large, generally leading to values for r significantly larger than 1, the form of the fluorescence quenching curves is not

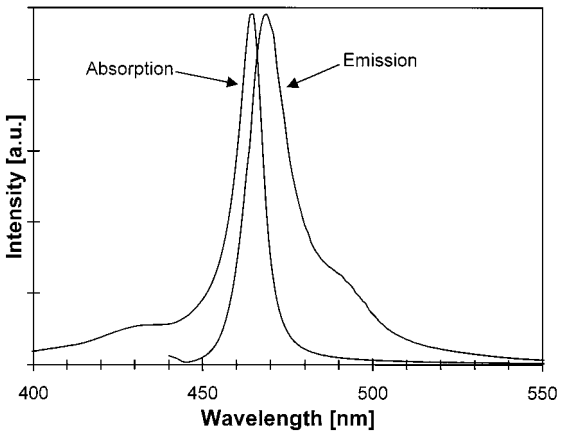

Figure 3. Steady-state absorption and emission ($\lambda_{exc} = 425$ nm) spectra of BTHC J-aggregate solution ($c_{dye} = 6.5 \times 10^{-5}$ M, $c_{NaCl} = 0.15$ M, in 1 mm cell) at room temperature. The peak optical density in this 1 mm sample was 1.62 at 465 nm..

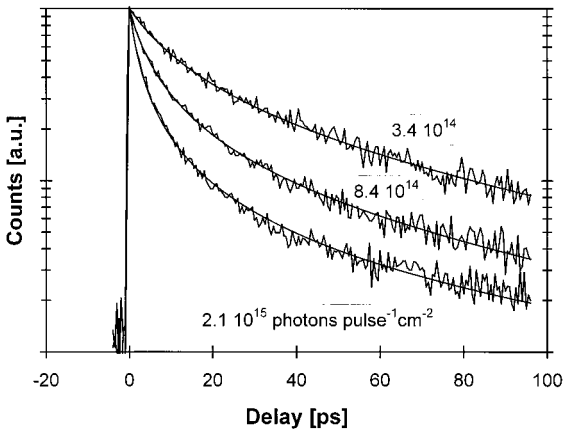

Figure 4. Fluorescence decay of BTHC at three different incident intensities as measured by fluorescence upconversion. Initial amplitudes of the curves are normalized for excitation intensity and integration times. Solid lines are fits of data to expression given in eq 1.

very sensitive to the value of r and only lower bounds on the domain size can be determined. In these cases, alternate units for the calculation of γ become more relevant.

Assuming that the excitons are localized, i.e., moving mainly by an incoherent hopping process that can be described as a two-dimensional random walk,[24] and considering only nearest-neighbor interactions, the exciton hopping rate k_h is to a first-order approximation given by[25]

$$k_h = \frac{1}{4}\left[\frac{\gamma}{2} D\left(\frac{\ln D}{\pi} + 0.195\right) - K\right] \qquad (6)$$

Derivation of eq 6 also assumes that every encounter of two excitons results in an annihilation, so that the estimate of k_h derived from this equation is a lower bound value.

Exciton Annihilation Results. Figure 3 illustrates the solution absorption and steady-state emission spectra of BTHC under the experimental conditions used for the exciton annihilation studies (6.5×10^{-5} M dye, 0.15 M NaCl, room temperature). As is usual in dilute, solution J-aggregates, the bandwidth of the J-band and the Stokes shift of the fluorescence are significantly smaller than for the monomeric dye. The low-intensity limit of the fluorescence decay rate was determined using TCSPC, which gave a value of 500 ± 20 ps for the fluorescence lifetime, $1/K$. This determination was used to fix K in the fits of the higher intensity fluorescence decay curves described below.

Figure 4 shows the fluorescence decay measured with fluorescence upconversion at three different excitation intensities and the corresponding fits using eq 1. The decays are clearly nonexponential and the quality of the fits is very good, confirming that eq 1 is a useful model for exciton-annihilation in BTHC J-aggregates. The good agreement of experiment and model is not surprising, since the aggregates we studied are two-dimensional; thus, the model assumptions are expected to be true for these aggregates. The agreement also indicates that r is in fact large, since that is the limit under which eq 1 was derived.

Over an intensity range of 3×10^{13} to 2.15×10^{15} photons pulse^{-1} cm^{-2}, the fits show that, as expected, $n(0)/r$ rises linearly even at very high excitation intensities, reaching a value of 264 ± 25 at the highest intensity. In addition, we did not observe a change in the initial amplitude of the fluorescence $I(t = 0)$ (normalized for the excitation intensity and the integration time), confirming that the measurements were always in a linear regime. To determine the value of r, we would next need to fit the experimental intensity dependence of the fluorescence quantum yield using eq 4. However, the nature of the upconversion experiments does not allow a direct measurement of the yield, since we are not able to measure the decay curve out to long times. Even with good data, determining r is difficult because the theoretical curves for the quantum yield change only slightly for $r > 2$. Since the limiting form of the decay curve fits our data so well, we can assume that a value of $r = 2$ is a lower limit and that a larger value of r is a strong possibility.

Although we cannot independently confirm the value of r, using $r \geq 2$ as an indication, we obtain an upper limit for the annihilation constant, $\gamma \leq 2 \times 10^9$ s^{-1}. From $n(0)/r = 264$ and $r \geq 2$, it also follows that 528 or more excitons are created in each domain at the highest excitation intensity. Knowing the sample concentration, optical density, laser power, and excited volume, we find that at this highest excitation power we create about one excitation in every 4 molecules, thus the domain size is greater than 2150 molecules (eq 5). Such a large domain size is consistent with the large 2D monolayer sheets expected for the smectic mesophase of this dye. It is also similar to the large domain size found by Sundström et al. for PIC J-aggregate,[13] greater than 15000 molecules per domain. Note that these domain sizes are much larger than the J-aggregation number deduced from older spectroscopic studies of monomer/J-aggregate "equilibria". As discussed by Herz,[3] these aggregation numbers relate approximately to the number of molecules undergoing the mutual spectral perturbation observed in the absorption spectrum, not to the actual physical size of the aggregates.

As part of this study of the femtosecond time-resolved fluorescence of the BTHC J-aggregate, we also examined the time evolution of the fluorescence at very short delay times in an attempt to obtain evidence for intraband relaxation in the J-aggregates. Since the excitation wavelength used in these studies is well above the bottom of the exciton band, this relaxation is predicted to give a time-dependent emission spectrum of the aggregate having additional short-lived and blue-shifted peaks apparent shortly after excitation.[27] In addition, a rise time is expected to be evident in the dominant emission from the bottom of the exciton band. We measured both time-resolved spectra at short delay times and fluorescence time evolution at different emission wavelengths between 430 and 550 nm using time increments as small as 20 fs. However, no evidence for time dependence in the emission spectrum was

TABLE 1: Exciton Annihilation Constant γ in Different Units for Three Cyanine Dyes

		BTHC		PIC		TDBC	
$n(t) =$	$[\gamma] =$	concentration (M)	γ	concentration (M)	γ	concentration (M)	γ
excitations/(domain× pulse)	domain s^{-1}	6.5×10^{-5}	$\leq 2 \times 10^{9}$	3×10^{-4}	$\leq 2 \times 10^{9}$ [13]		
excitations/($cm^3 \times$ pulse)	$cm^3\ s^{-1}$	6.5×10^{-5}	1.03×10^{-4}	3×10^{-4}	2.6×10^{-3}[13]	5×10^{-5}	1.02×10^{-3} [14]
				3×10^{-4}	1.7×10^{-4}[13[c]]		
				1×10^{-2}	3.1×10^{-6}[11[a]]		
excitations/(illuminated area × pulse)	$cm^2\ s^{-1}$	6.5×10^{-5}	1.03×10^{-2}	1×10^{-2}	1.2×10^{-2}[11[a]]		
				1×10^{-2}	8×10^{-3}[12[e]]		
excitations/(molecule × pulse)	molecule s^{-1}	6.5×10^{-5}	4.27×10^{12}	3×10^{-4}	4.7×10^{14}[13[b]]	5×10^{-5}	3.1×10^{13} [14[d]]
				3×10^{-4}	3.0×10^{13}[13[c]]		
				1×10^{-2}	1.9×10^{13}[11[a]]		
				1×10^{-2}	1.6×10^{13}[12[f]]		

[a] Recalculated from ref 11 using original data, see text. [b] Calculated from ref 13 using 2.6×10^{-3} $cm^3\ s^{-1}$ value of γ and values for solution parameters given in reference. [c] Calculated from ref 13 using fluorescence quenching data and values for solution parameters, see text. [d] Calculated from ref 14 using 1.02×10^{-3} $cm^3\ s^{-1}$ value of γ and values for solution parameters given in reference. [e] Calculated from ref 12 increasing value for γ by 4 times to account for difference in definition. [f] Calculated from ref 12 using 8×10^{-3} $cm^2\ s^{-1}$ value of γ and values for solution parameters given in reference.

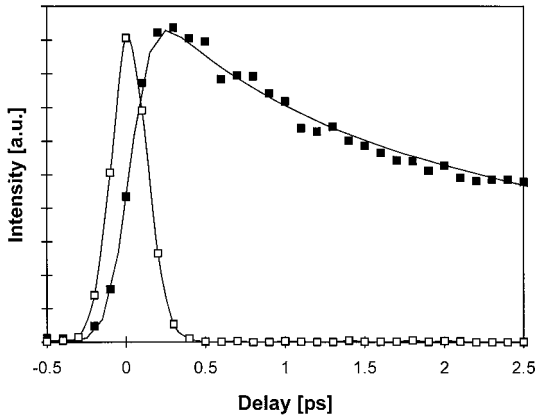

Figure 5. System response (cross-correlation of the two laser beams) and fluorescence decay at short times (2.02×10^{15} photons $pulse^{-1}$ cm^{-2}) fitted with the convolution of the system response with the expression given in eq 1.

found. Further, as shown in Figure 5, even at very short times, we were able to fit the upconversion data for fluorescence at 470 nm with a convolution of the cross-correlation of the two laser beams with the exciton−annihilation model given by eq 1. This result indicates that there is no rise-time component evident in the emission from the bottom of the band. Consequently, we conclude that intraband relaxation in this system occurs on a faster time scale than 100 fs, the approximate time resolution of our apparatus. It is also worth noting that we did not observe the deviation from the exciton annihilation model at very short times reported by van Burgel et al.[14] for grating scattering experiments on TDBC aggregates.

For comparisons of the value of the exciton annihilation constant γ obtained for BTHC with those for previously studied J-aggregates, we first note that $\gamma n(0)$ $(= (n(0)/r)2K)$ can be experimentally determined without knowledge of the value of r (at our highest intensity $\gamma n(0) = (1.06 \pm 0.07) \times 10^{12}\ s^{-1}$). This fact can be used to compare previously reported values for γ by considering the different definitions used for the excitation density $n(t)$. In previous publications, $n(t)$ has been defined as the number of excitations per domain, the number of excitations per unit volume (refs 13, 14, and 19), or the number of excitations per area illuminated by the laser (refs 11 and 12). In Table 1, we show the results for BTHC in the different units and compare them to previously reported values for the J-aggregates of PIC and TDBC. As part of the Table, we have also included values from our earlier work on PIC,[11] recalculated in the various units, using the original data.[28]

However, considering the problems in determining the domain size and the fact that comparison in terms of excitations per volume or area can be somewhat misleading for heterogeneous solutions of different concentration, we propose yet another set of units for $n(t)$: that of number of excitations per molecule. This value can be determined from the concentration and optical density of the sample, the laser power, and the excited volume. We have included the resulting value for γ (in units of molecule s^{-1}) in the last row of Table 1, converting the data of other workers to these units where possible.

In comparing the values of γ for PIC in these new units, we were surprised to note the more than a factor of 10 difference between our value, based on ref 11 and the value derived from the absorption recovery kinetics measurements of Sundström and co-workers in ref 13. The Sundström work studied the exciton annihilation by two different techniques: absorption recovery kinetics, which gave a value of $\gamma = 2.6 \times 10^{-3}$ cm^3 s^{-1}, and fluorescence quenching, which was analyzed using the excitations/domain approach and gave a value of $\gamma \leq 2 \times 10^{9}$ domain s^{-1}. However, the fluorescence quenching data of Sundström can also be reanalyzed in terms of excitations/solution volume or excitations/molecule. In Figure 4 of ref 13, the fluorescence is seen to be 50% quenched at an excitation intensity of 5×10^{12} absorbed photons $pulse^{-1}$ cm^{-2}. In this case, using our eq 3 and data given in ref 13 for the optical cell thickness and the solution concentration and optical density, values of $\gamma = 1.7 \times 10^{-4}$ $cm^3\ s^{-1}$ or $\gamma = 3.0 \times 10^{13}$ molecule s^{-1} are obtained. While it is not clear why Sundström's two experimental techniques should give such different values for γ, the value of γ from the reanalyzed fluorescence quenching data is nearly the same as the value obtained from our earlier PIC data and the value obtained by Stiel et al.,[12] when units of molecule s^{-1} are used. Thus, we choose to consider the value of γ derived from the fluorescence quenching data as the appropriate number to compare with other values determined by fluorescence techniques. This agreement also supports the validity of using the molecule s^{-1} units when comparing solutions of different concentration and/or different sample thickness.

Comparing the annihilation data in terms of molecule s^{-1} for

the three dyes summarized in Table 1 reveals that the annihilation constants for PIC and TDBC are quite similar, while the constant for BTHC is lower by a factor of 5−8 times. For evaluating differences in γ, the approximately 2-fold variation in the value of γ obtained from the various PIC fluorescence measurements suggests that, as discussed previously, obtaining exact agreement between values of γ in different experiments requires careful attention to the sample phase equilibria and the experimental protocol employed for studying J-aggregated dye liquid crystals, particularly the *nematic* type. Furthermore, using the data normalization approach adopted here (molecule s^{-1}), it may be critical to estimate, and correct for, the concentration of any coexisting non-J-aggregated dye solution species, particularly for temperature-sensitive phase equilibria with dyes such as PIC. Such corrections have not been applied to the PIC compositions in this instance, while BTHC and TDBC both exhibit vanishingly low monomer concentrations as studied, and should be little affected. Despite these considerations, the value obtained for γ for the BTHC aggregates is enough smaller than the values for PIC and TDBC to be a difference that is outside expected experimental corrections. The earlier discussion indicates that this difference cannot be correlated simply with the mesophase structural type and associated J-aggregate architecture for the specific sample compositions studied (i.e., nematic columnar dye aggregates for PIC versus smectic 2D layered dye aggregates for both BTHC and TDBC-1).

The differences in γ for the three dyes can be approximately translated into exciton hopping rates using eq 6. The required value for $D\gamma$ can be calculated from $n(0)\gamma$ divided by the fraction F of molecules excited, and for large values of the domain size D, the ln D term is quite insensitive to the value assumed for D. Using $D = 2000$ molecules for this estimate (the lower bound for our BTHC measurement and a conservative value for a smectic J-aggregate), values of k_h become 1×10^{12} s^{-1} for BTHC, 5 to 9×10^{12} s^{-1} for PIC, and 9×10^{12} s^{-1} for TDBC.

Another aspect to be considered in discussions of exciton mobility differences is the extent of short-range disorder within the J-aggregate structure. Disorder is expected to lower exciton mobility by perturbing the exact energetic equivalence between adjacent molecules.[29] The bandwidth of the J-aggregate peak is one indication of such disorder. Examining the half bandwidths for the three different aggregates reveals that BTHC has the largest width, 570 cm^{-1}, compared with 240 cm^{-1} for TDBC and 130 cm^{-1} for PIC. Since BTHC and TDBC both form smectic-mesophase J-aggregates, it is reasonable to assume that this ∼2× difference in bandwidth reflects differences in short-range disorder that are large enough to cause significant differences in exciton mobility, as observed. Continuing this argument, the very narrow bandwidth seen for PIC might be expected to give the largest observed exciton mobility. However, in this case, the fundamentally different structure of the mesogenic PIC J-aggregates makes this expectation questionable and indeed, the exciton mobility derived for PIC is no larger than that obtained for TDBC. In addition, the derivation of exciton mobility from γ using eq 6 requires the assumption that there is unit probability of annihilation for every exciton−exciton encounter. Thus, in discussing differences in exciton mobility between the PIC J-aggregates and the BTHC and TDBC J-aggregates, a further complication is a possible difference in annihilation probability for excitons in the columnar PIC aggregate compared with those in the layered 2D BTHC and TDBC aggregate structures.

Summary and Conclusions

Using a fluorescence upconversion apparatus with 100 fs time resolution, the time-dependent fluorescence decay of BTHC J-aggregates stabilized in aqueous 0.15 M NaCl solution was examined at various excitation intensities. Over a range of 3×10^{13} to 2.12×10^{15} photons $pulse^{-1}$ cm^{-2}, the fluorescence decay is well described by the singlet−singlet exciton annihilation model of Paillotin et al. Under the assumptions of the model, the upper limit for the exciton annihilation constant is 2×10^9 domain $s^{-1}$and the exciton domain size is greater than 2150 molecules. This size is large enough that the exciton annihilation kinetics are essentially unperturbed by any restrictions relating to domain size. Attempts to time-resolve spectral features related to intraband relaxation in the excited excitonic states of the BTHC J-aggregate prior to annihilation indicate that these relaxation processes are faster than 100 fs at room temperature.

The large domain size obtained for the BTHC J-aggregate is consistent with the smectic liquid-crystalline nature of the dye, as studied. Here, the individual mesogenic J-aggregates are "infinitely extending" 2D sheets or layers of monomolecular thickness.[6] The liquid crystalline behavior of two other cyanine J-aggregates for which exciton annihilation has been previously studied was also examined, so that possible correlations between annihilation rates and mesoscopic structure of the specific dye solutions could be discussed. The annihilation rate for the BTHC smectic J-aggregates is nearly 1 order of magnitude lower than those reported for the (liquid-crystalline, 2D smectic) J-aggregates of TDBC and the (liquid-crystalline, columnar nematic) J-aggregates of PIC, when compared in units of molecule s^{-1}. For the BTHC to TDBC comparison, where the liquid-crystalline structures are similar, this difference can be rationalized as the result of a difference in short range disorder, as reflected in the 2× broader bandwidth of the BTHC aggregate. For the BTHC to PIC comparison, disorder is one potential factor influencing the annihilation rate, but the difference in liquid crystalline structure may also play a significant role. Further comparative studies of cyanine dye smectic and nematic J-aggregated mesophases are clearly necessary to further improve our understanding of excitation transport in these complex self-assembled colloidal systems.

Acknowledgment. We are grateful to the National Science Foundation for a Science and Technology Center grant, CHE-8810024, to J. Lanzafame for the initial setup of the fluorescence upconversion experiment, to S. Diol for support doing the TCSPC experiments, and to David K. Foster for polarized absorption measurements.

References and Notes

(1) Special Issue: Optics of Nanostructures. *Phys. Today* **1993**, *46*.
(2) Dähne, S.; De Rossi, U.; Moll, J. *J. Soc. Photogr. Sci. Technol. Jpn.* **1996**, *59*, 250−259.
(3) Herz, A. H. *Adv. Colloid Interface Sci.* **1977**, *8*, 237.
(4) Davydov, A. S. *Theory of Molecular Excitons*; Plenum Press: New York, 1971.
(5) James, T. H. *The Theory of the Photographic Process*, 4th ed.; Macmillan: New York, 1977.
(6) Harrison, W. J.; Mateer, D. L.; Tiddy, G. J. T. *J. Phys. Chem.* **1996**, *100*, 2310.
(7) Tiddy, G. J. T.; Mateer, D. L.; Ormerod, A. P.; Harrison, W. J.; Edwards, D. J. *Langmuir* **1995**, *11*, 390.
(8) Attwood, T. K.; Lydon, J. E. *Liq. Cryst.* **1986**, *1*, 499.
(9) Sadler, D. E.; Shannon, M. D.; Tollin, P.; Young, D. W.; Edmondson, M.; Rainsford, P. *Liq. Cryst.* **1986**, *1*, 509.
(10) Stegemeyer, H.; Stockel, F. *Ber. Bunsen-Ges. Phys. Chem.* **1996**, *100*, 9.

(11) Brumbaugh, D. V.; Muenter, A. A.; Knox, W.; Mourou, G.; Wittmershaus, B. *J. Lumin.* **1984**, *31/32*, 783.

(12) Stiel, H.; Dähne, S.; Teuchner, K. *J. Lumin.* **1988**, *39*, 351.

(13) Sundström, V.; Gillbro, T.; Gadonas, R. A.; Piskarskas, A. *J. Chem. Phys*. **1988**, *89*, 2754.

(14) van Burgel, M.; Wiersma, D. A.; Duppen, K. *J. Chem. Phys*. **1995**, *102*, 20.

(15) Harrison, W. J.; Mateer, D. L.; Tiddy, G. J. T. *Faraday Discuss.* **1996**, *104*.

(16) Reid, P. J.; Higgins, D. A.; Barbara, P. F. *J. Phys. Chem*. **1996**, *100*, 3892.

(17) Harrison, W. J.; Tiddy, G. J. T.; Mateer, D. L.; Bottrill, C. J. Unpublished results.

(18) Crowley, T. L.; Bottrill, C.; Mateer, D.; Harrison, W. J.; Tiddy, G. J. T. *Colloids Surf. A* **1997**, *129*−*130*, 95.

(19) Paillotin, G.; Swenberg, C. E.; Breton, J.; Geacintov, N. E. *Biophys. J.* **1979**, *25*, 513.

(20) Swenberg, C. E.; Geacintov, N. E.; Pope, M. *Biophys. J*. **1976**, *16*, 1447.

(21) Dexheimer, S. L.; Vareka, W. A.; Mittleman, D.; Zettl, A.; Shank, C. V. *Chem. Phys. Lett*. **1995**, *235*, 552.

(22) Kopelman, R.; Parus, S. J.; Prasad, J. *Chem. Phys*. **1988**, *128*, 209.

(23) Pfeifer, P.; Obert, M. *In The Fractal Approach to Heterogeneous Chemistry*; Avnir, D. Ed.; Wiley: Chichester, 1989; Chapter 11.

(24) Montroll, E. W. *J. Math. Phys*. **1969**, *10*, 753.

(25) den Hollander, W. T.F.; Bakker, J. G. C.; van Grondelle, R. *Biochim. Biophys. Acta* **1983**, *725*, 492.

(26) Although 425 or 427 nm would also excite any monomers or H-aggregates present in the J-aggregate sample, the studies of the J-aggregate smetic mesophase under these conditions show minimal concentration of monomer or H-aggregate in equilibrium with the mesophase. In addition, steady-state luminescence measurements of monomer/H-aggregate solutions of BTHC indicate a fluorescence yield at least 2 orders of magnitude lower than the J-aggregate. Consequently, no interference from monomer or H-aggregate emission is expected in the time-resolved fluorescence measurements.

(27) Chernyak, V.; Wang, N.; Mukamel, S. *Phys. Rev*. **1995**, *263*, 213.

(28) The definition of γ in ref 1 omitted the factor of $^1/_2$ in eq 2. The value given in Table 1 has been corrected for this factor.

(29) Förster, T. *Ann. Phys.* **1948**, *2*, 55.